A computational and theoretical analysis on the two-dimensional Vicsek model.

Matthijs Cornelis den Heijer

Statistical physics b
Leiden University

Leiden, Monday 28th April, 2025

Supervisor: Dr. L. Giomi

Contents

1. Introduction

The Vicsek model is a mathematical model used to study the collective behaviour of self-propelled particles, such as birds in a flock or fish in a school. The model simulates the motion of particles, each individual particle is influenced by the motion of its nearby neighbors. This behaviour leads to collective motion of grouped particles. The particles in the model will be limited to two spatial dimensions. The model comes with its limitations, which become clear in the conclusion and discussion section. The goal of the report is to study the complex behaviour of the Vicsek model in two dimensions and to find the critical scaling exponent using computational and theoretical methods. The computational method consists of a simulation program provided by Leiden University. The data of the simulation is analysed by a selfmade Python code.

This report is part of the Statistical physics b program, done at the department of Physics at Leiden University as part of the Masters course.

2. Theory

Consider a simple model that describes the collective motion of a multi particle system in two dimensions. The collection of particles propel themselves forward through space by converting stored energy into motion. The number of active particles in a region with volume l^d in d dimensions is given by,

$$N = \int d\boldsymbol{r}\rho, \tag{1}$$

where ρ is the number density in the region. The standard deviation in the number of particles is related to the average number of particles in the region by, the scaling law:

$$\Delta N \sim \langle N \rangle^z, \tag{2}$$

where z is the critical exponent. Finding this exponent will be the priority of this research project. As the particles propagate through space, neighbouring particles should (slowly) align themselves with the average orientation of the system with some random noise in their orientation. The model that describes this motion is the Vicsek model. According to the Vicsek model in the continuous limit, the evolution of the number density and their orientation is described by:

$$\partial_t \rho = D\nabla^2 \rho - v_0 \nabla \cdot (\rho \boldsymbol{p}), \tag{3a}$$
$$\partial_t \theta = D_r \nabla^2 \theta + \xi, \tag{3b}$$

where $\boldsymbol{p} = \cos\theta \hat{\boldsymbol{x}} + \sin\theta \hat{\boldsymbol{y}}$ is the local polarization with θ the orientation field, D, D_r and v_0 are constants, ξ denotes an uncorrelated random field, such that

$$\langle \xi(\boldsymbol{r}, t) \rangle = 0, \quad \langle \xi(\boldsymbol{r}, t) \xi(\boldsymbol{r}', t') \rangle = \Delta \delta(\boldsymbol{r} - \boldsymbol{r}') \delta(t - t'), \tag{4}$$

where Δ is a constant. The Laplacian terms ensure that over time, the system will go towards its local minimum point i.e. all the particles will align accordingly so that the orientation field is minimized. The divergence term ensures that the particles will not diverge far from one another and attract the particles together. The constant v_0 gives the particles a self-propellant velocity. Perturbing the number density and orientation field near their average by taking $\rho(\boldsymbol{r}, t) = \langle \rho \rangle + \delta\rho(\boldsymbol{r}, t)$ and $\theta(\boldsymbol{r}, t) = \langle \theta \rangle + \delta\theta(\boldsymbol{r}, t)$. Then,

$$\partial_t (\langle \rho \rangle + \delta\rho(\boldsymbol{r}, t)) = D\nabla^2 (\langle \rho \rangle + \delta\rho(\boldsymbol{r}, t)) - v_0 \nabla \cdot ((\langle \rho \rangle + \delta\rho(\boldsymbol{r}, t)) \boldsymbol{p}), \tag{5a}$$
$$\partial_t (\langle \theta \rangle + \delta\theta(\boldsymbol{r}, t)) = D_r \nabla^2 (\langle \theta \rangle + \delta\theta(\boldsymbol{r}, t)) + \xi. \tag{5b}$$

Since the averages $\langle \rho \rangle$ and $\langle \theta \rangle$ are time-and space-independent, the formulae reduce to:

$$\partial_t \delta\rho = D\nabla^2 \delta\rho - v_0 \nabla \cdot ((\langle \rho \rangle + \delta\rho) \boldsymbol{p}), \tag{6a}$$
$$\partial_t \delta\theta = D_r \nabla^2 \delta\theta + \xi. \tag{6b}$$

Without loss of generality, set $\langle \theta \rangle = 0$. Note that the perturbation $\delta\theta$ is very small, applying a Taylor expansion to $\boldsymbol{p}$ up to the first order, gives

$$\boldsymbol{p} \approx \hat{\boldsymbol{x}} + \delta\theta \hat{\boldsymbol{y}}. \tag{7}$$

Therefore the divergence in 6a becomes,

$$\nabla \cdot ((\langle\rho\rangle + \delta\rho)(\hat{\boldsymbol{x}} + \delta\theta\hat{\boldsymbol{y}}) = \partial_x\delta\rho + \langle\rho\rangle\partial_y\delta\theta. \tag{8}$$

Then the evolution of the small perturbation terms $\delta\rho$ and $\delta\theta$ read,

$$\partial_t\delta\rho = D\nabla^2\delta\rho - v_0\left(\partial_x\delta\rho + \langle\rho\rangle\partial_y\delta\theta\right), \tag{9a}$$
$$\partial_t\delta\theta = D_r\nabla^2\delta\theta + \xi. \tag{9b}$$

In Fourier space,

$$\delta\theta(\boldsymbol{r},t) = \frac{1}{l^d}\sum_{\boldsymbol{q}}\int\frac{d\omega}{2\pi}\delta\theta_{\boldsymbol{q}}(\omega)e^{i(\boldsymbol{q}\cdot\boldsymbol{r}-\omega t)}, \tag{10a}$$

$$\delta\rho(\boldsymbol{r},t) = \frac{1}{l^d}\sum_{\boldsymbol{q}}\int\frac{d\omega}{2\pi}\delta\rho_{\boldsymbol{q}}(\omega)e^{i(\boldsymbol{q}\cdot\boldsymbol{r}-\omega t)}, \tag{10b}$$

$$\xi(\boldsymbol{r},t) = \frac{1}{l^d}\sum_{\boldsymbol{q}}\int\frac{d\omega}{2\pi}\xi_{\boldsymbol{q}}(\omega)e^{i(\boldsymbol{q}\cdot\boldsymbol{r}-\omega t)}. \tag{10c}$$

Using the following mathematical tools, to Fourier transform the evolution equations of the system,

$$\partial_t\delta\rho(\boldsymbol{r},t) = \frac{1}{l^d}\sum_{\boldsymbol{q}}\int\frac{d\omega}{2\pi}(-i\omega)\delta\rho_{\boldsymbol{q}}(\omega)e^{i(\boldsymbol{q}\cdot\boldsymbol{r}-\omega t)}, \tag{11a}$$

$$\nabla^2\delta\rho(\boldsymbol{r},t) = \frac{1}{l^d}\sum_{\boldsymbol{q}}\int\frac{d\omega}{2\pi}(-|\boldsymbol{q}|^2)\delta\rho_{\boldsymbol{q}}(\omega)e^{i(\boldsymbol{q}\cdot\boldsymbol{r}-\omega t)}, \tag{11b}$$

$$\partial_x\delta\rho(\boldsymbol{r},t) = \frac{1}{l^d}\sum_{\boldsymbol{q}}\int\frac{d\omega}{2\pi}(iq_x)\delta\rho_{\boldsymbol{q}}(\omega)e^{i(\boldsymbol{q}\cdot\boldsymbol{r}-\omega t)}, \tag{11c}$$

$$\partial_y\delta\rho(\boldsymbol{r},t) = \frac{1}{l^d}\sum_{\boldsymbol{q}}\int\frac{d\omega}{2\pi}(iq_y)\delta\rho_{\boldsymbol{q}}(\omega)e^{i(\boldsymbol{q}\cdot\boldsymbol{r}-\omega t)}. \tag{11d}$$

Similarly for $\delta\theta$,

$$\partial_t\delta\theta(\boldsymbol{r},t) = \frac{1}{l^d}\sum_{\boldsymbol{q}}\int\frac{d\omega}{2\pi}(-i\omega)\delta\theta_{\boldsymbol{q}}(\omega)e^{i(\boldsymbol{q}\cdot\boldsymbol{r}-\omega t)}, \tag{12a}$$

$$\nabla^2\delta\theta(\boldsymbol{r},t) = \frac{1}{l^d}\sum_{\boldsymbol{q}}\int\frac{d\omega}{2\pi}(-|\boldsymbol{q}|^2)\delta\theta_{\boldsymbol{q}}(\omega)e^{i(\boldsymbol{q}\cdot\boldsymbol{r}-\omega t)}. \tag{12b}$$

In Fourier space, equation 9 becomes,

$$-i\omega\delta\rho_{\boldsymbol{q}}(\omega) = -D|\boldsymbol{q}|^2\delta\rho_{\boldsymbol{q}}(\omega) - iv_0\left(q_x\delta\rho_{\boldsymbol{q}}(\omega) + \langle\rho\rangle q_y\delta\theta_{\boldsymbol{q}}(\omega)\right), \tag{13a}$$
$$-i\omega\delta\theta_{\boldsymbol{q}}(\omega) = -D_r|\boldsymbol{q}|^2\delta\theta_{\boldsymbol{q}}(\omega) + \xi_{\boldsymbol{q}}(\omega). \tag{13b}$$

Rewriting in terms of $\rho_{\boldsymbol{q}}(\omega)$ and $\theta_{\boldsymbol{q}}(\omega)$,

$$\delta\rho_{\boldsymbol{q}}(\omega) = \frac{-iv_0\langle\rho\rangle q_y\delta\theta_{\boldsymbol{q}}(\omega)}{D|\boldsymbol{q}|^2 + iv_0q_x - i\omega}, \tag{14a}$$

$$\delta\theta_{\boldsymbol{q}}(\omega) = \frac{\xi_{\boldsymbol{q}}(\omega)}{-i\omega + D_r|\boldsymbol{q}|^2}. \tag{14b}$$

The variance of the number density is related to the correlation function by,

$$\langle \delta\rho_{\boldsymbol{q}}(\omega)\delta\rho_{\boldsymbol{q'}}\left(\omega'\right)\rangle = 2\pi\ell^d\Delta\rho^2_{\boldsymbol{q}}(\omega)\delta_{\boldsymbol{q},-\boldsymbol{q'}}\delta\left(\omega+\omega'\right). \tag{15}$$

Before computing the number density variance, firstly Fourier transform the uncorrelated random field,

$$\begin{aligned}
\langle \xi_{\boldsymbol{q}}(\omega)\xi_{\boldsymbol{q'}}(\omega')\rangle &= \langle \int dtdt'd\boldsymbol{r}d\boldsymbol{r'}\xi(\boldsymbol{r},t)\xi\left(\boldsymbol{r'},t'\right)e^{i(\boldsymbol{q'}\cdot\boldsymbol{r'}-\omega't')}e^{i(\boldsymbol{q}\cdot\boldsymbol{r}-\omega t)}\rangle \\
&= \int dtdt'd\boldsymbol{r}d\boldsymbol{r'}\Delta\delta\left(\boldsymbol{r}-\boldsymbol{r'}\right)\delta\left(t-t'\right)e^{i(\boldsymbol{q'}\cdot\boldsymbol{r'}-\omega't')}e^{i(\boldsymbol{q}\cdot\boldsymbol{r}-\omega t)} \\
&= \int dtd\boldsymbol{r}\Delta e^{i(\boldsymbol{q'}\cdot\boldsymbol{r}-\omega't)}e^{i(\boldsymbol{q}\cdot\boldsymbol{r}-\omega t)} \\
&= 2\pi l^d\Delta\delta_{\boldsymbol{q},-\boldsymbol{q'}}\delta(\omega+\omega'),
\end{aligned} \tag{16}$$

where in the last line

$$\int d\boldsymbol{r}e^{-i(\boldsymbol{q}+\boldsymbol{q'})\boldsymbol{r}} = 2\pi^d\delta(\boldsymbol{q}+\boldsymbol{q'}) \to l^d\delta_{\boldsymbol{q},-\boldsymbol{q'}}. \tag{17}$$

Then the correlation function of the orientation field is,

$$\begin{aligned}
\langle \delta\theta_{\boldsymbol{q}}(\omega)\delta\theta_{\boldsymbol{q'}}(\omega')\rangle &= \langle \frac{\xi_{\boldsymbol{q}}(\omega)}{-i\omega+D_r\left|\boldsymbol{q}\right|^2}\frac{\xi_{\boldsymbol{q'}}(\omega')}{-i\omega'+D_r\left|\boldsymbol{q'}\right|^2}\rangle \\
&= \frac{2\pi l^d\Delta\delta_{\boldsymbol{q},-\boldsymbol{q'}}\delta(\omega+\omega')}{(-i\omega+D_r\left|\boldsymbol{q}\right|^2)(-i\omega'+D_r\left|\boldsymbol{q'}\right|^2)}
\end{aligned} \tag{18}$$

Combining Eqs. (14), (15) and (18),

$$\begin{aligned}
&\langle \delta\rho_{\boldsymbol{q}}(\omega)\delta\rho_{\boldsymbol{q'}}(\omega')\rangle = 2\pi l^d\Delta\rho^2_{\boldsymbol{q}}(\omega)\delta_{\boldsymbol{q},-\boldsymbol{q'}}\delta\left(\omega+\omega'\right) \\
&= \langle \frac{-iv_0\langle\rho\rangle q_y\delta\theta_{\boldsymbol{q}}(\omega)}{D\left|\boldsymbol{q}\right|^2+iv_0q_x-i\omega}\frac{-iv_0\langle\rho\rangle q'_y\delta\theta_{\boldsymbol{q'}}(\omega')}{D\left|\boldsymbol{q'}\right|^2+iv_0q'_x-i\omega'}\rangle \\
&= \frac{-v_0^2\langle\rho\rangle^2q_yq'_y2\pi l^d\Delta\delta_{\boldsymbol{q},-\boldsymbol{q'}}\delta(\omega+\omega')}{(-i\omega+D_r\left|\boldsymbol{q}\right|^2)(-i\omega'+D_r\left|\boldsymbol{q'}\right|^2)(D\left|\boldsymbol{q}\right|^2+iv_0q_x-i\omega)(D\left|\boldsymbol{q'}\right|^2+iv_0q'_x-i\omega')}
\end{aligned} \tag{19}$$

Integrating the right hand-side of the first line and the last line over ω' and summing over all $\boldsymbol{q'}$, gives

$$\begin{aligned}
\Delta\rho^2_{\boldsymbol{q}}(\omega) &= \frac{v_0^2\langle\rho\rangle^2q_y^2\Delta}{(-i\omega+D_r\left|\boldsymbol{q}\right|^2)(i\omega+D_r\left|\boldsymbol{q}\right|^2)(D\left|\boldsymbol{q}\right|^2+iv_0q_x-i\omega)(D\left|\boldsymbol{q}\right|^2-iv_0q_x+i\omega)} \\
&= \frac{v_0^2\langle\rho\rangle^2q_y^2\Delta}{(\omega^2+D_r^2\left|\boldsymbol{q}\right|^4)(D^2\left|\boldsymbol{q}\right|^4+(v_0q_x-\omega)^2)}
\end{aligned} \tag{20}$$

Looking at the limit where the particles have infinite velocity, the number density variance becomes,

$$\begin{aligned}
\Delta\rho^2_{\boldsymbol{q}}(\omega) &= \lim_{v_0\to\infty}\frac{\langle\rho\rangle^2q_y^2\Delta}{(\omega^2+D_r^2\left|\boldsymbol{q}\right|^4)(q_x^2+\frac{D^2|\boldsymbol{q}|^4-2q_x\omega^2v_0+\omega^2}{v_0^2})} \\
&= \frac{\langle\rho\rangle^2\Delta}{\omega^2+D_r^2\left|\boldsymbol{q}\right|^4}\left(\frac{q_y}{q_x}\right)^2
\end{aligned} \tag{21}$$

This result will be used to determine the z-exponent. In this model, the number density fluctuations can be calculated by

$$\Delta N = \lim_{q\to 0} \sqrt{\ell^d \int_{-\infty}^{\infty} \frac{\mathrm{d}\omega}{2\pi} \Delta\rho_{\boldsymbol{q}}^2(\omega)} \tag{22}$$

Calculating the integral inside the square root, with the number density variance of Eq. (21),

$$\int_{-\infty}^{\infty} \frac{d\omega}{2\pi} \frac{\langle\rho\rangle^2\Delta}{\omega^2 + D_r^2 \left|\boldsymbol{q}\right|^4} \left(\frac{q_y}{q_x}\right)^2 = \frac{1}{2\pi} \frac{\pi\langle\rho\rangle\Delta}{D_r \left|\boldsymbol{q}\right|^2} \left(\frac{q_y}{q_x}\right)^2 \tag{23}$$

Using the fact that, $q = \frac{2\pi}{l}$, and the result of the integral, the number density fluctuations becomes

$$\begin{aligned} \Delta N &= \lim_{q\to 0} \sqrt{l^d \frac{1}{2\pi} \frac{\pi\langle\rho\rangle\Delta}{D_r \left|\boldsymbol{q}\right|^2} \left(\frac{q_y}{q_x}\right)^2} \\ &\propto \lim_{q\to 0} l^{d/2+1} \end{aligned} \tag{24}$$

Using the scaling law of Eq. (2) and the fact that, $\langle N\rangle \approx \langle\rho\rangle l^d$, gives the final relation to determine the z exponent,

$$\frac{1}{d}\left(\frac{d}{2}+1\right) = z \tag{25}$$

In two-dimensions, $d = 2$, the final result is $z = 1$. However this result is only true for a system that has a sufficiently small noise term. In systems where the noise term dominates, the particles are unable to align their orientation, and so cannot behave as a collective group. The number density variance becomes,

$$\langle\delta\rho_{\boldsymbol{q}}(\omega)\delta\rho_{\boldsymbol{q'}}(\omega')\rangle \sim \frac{1}{|q|^{\alpha}}, \tag{26}$$

where $\alpha = 0$. Repeating a similar calculation, gives

$$\frac{1}{2d}\left(d+\alpha\right) = z. \tag{27}$$

Therefore in a noise dominated region, the z-exponent is $z = \frac{1}{2}$.

3. Experimental

3.1. Method

For every simulation, the number of particles is $N = 2000$, the number of simulation steps performed is 5000, the constant $v_0 = 0.03$ and the particle density is $\rho = 5$. Different values of η (noise) are taken for a full analysis of the system, this η represents a noise term in the orientation of the particles. The initial positions and orientation for every particle is randomized. After the simulation has completed, the results consist of the average polarization measured at different simulation steps, and a set of N in regions of decreasing size. For a correct analysis, the system must first be thermalized. To determine various quantities (with their respective errors) of the system, the correlation time is required. The time it takes for the system to be thermalized (correlation time) is calculated using an auto-correlation function,

$$\begin{aligned}\chi(t) =& \frac{1}{\Delta\theta}\left[\frac{1}{t_{\max}-t}\sum_{t'=0}^{t_{\max}-t}\theta\left(t'\right)\theta\left(t'+t\right)\right. \\ &\left. -\frac{1}{t_{\max}-t}\sum_{t'=0}^{t_{\max}-t}\theta\left(t'\right)\times\frac{1}{t_{\max}-t}\sum_{t'=0}^{t_{\max}-t}\theta\left(t'+t\right)\right].\end{aligned} \tag{28}$$

The system is thermalized when the auto-correlation function reaches a near zero value for the first time.

3.2. Results

Firstly, an analysis for a sufficiently low noise value $\eta = 0.30$ is performed, which lies in the ordered phase of the system. The auto correlation time is determined using Eq. (28) for the average polarisation of the system. Figure (1), shows the auto-correlation function for a single simulation for $\eta = 0.30$.

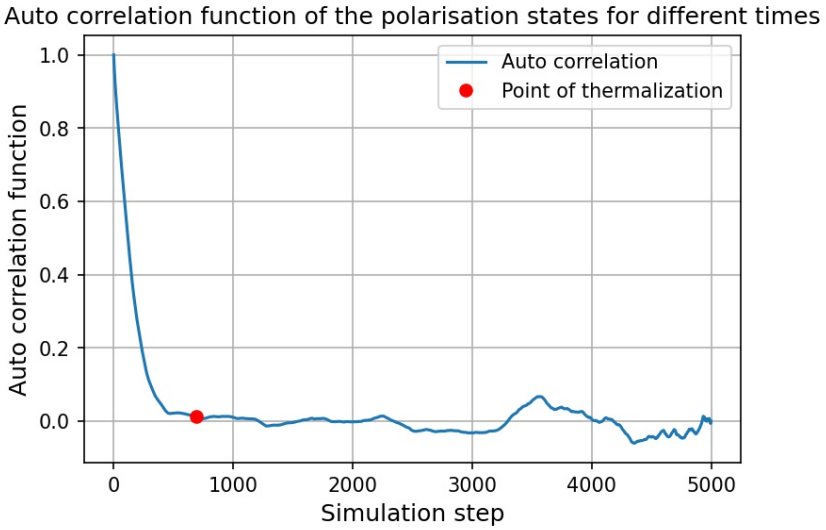

Figure 1: The auto-correlation function of $\eta = 0.30$. The red dot represents the simulation step at which the system has reached thermalization.

Due to the noise in the system, the auto-correlation function will fluctuate near zero in the ordered phase. All measurements for the set of N in regions of decreasing size are performed from the point of thermalization. Figure (2), shows the $\log(\langle N \rangle)$ vs $\log(\Delta N)$ plot.

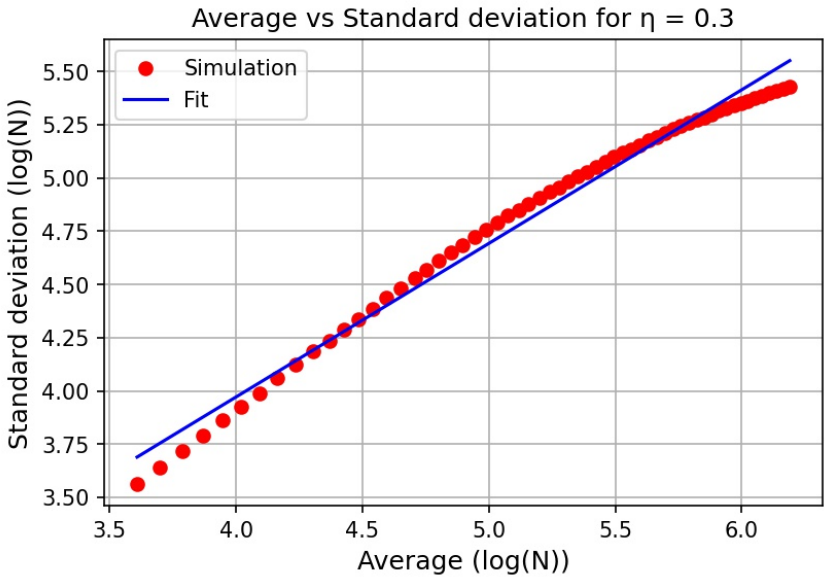

Figure 2: The log-log plot of the average vs the standard deviation for $\eta = 0.30$. The red dots represent the simulation data. The blue line represents the fit of the simulation data.

The fit closely represents the simulation data. The slope of the fit indicates the critical exponent z, which is $z = 0.72$.

Secondly, for a sufficiently high noise value, $\eta = 0.80$, the system will be in the disordered phase. In the disordered phase, the noise dominates and thus the average orientation at each simulation step will be uncorrelated. Figure (3), shows the auto-correlation function for a noise value of $\eta = 0.80$.

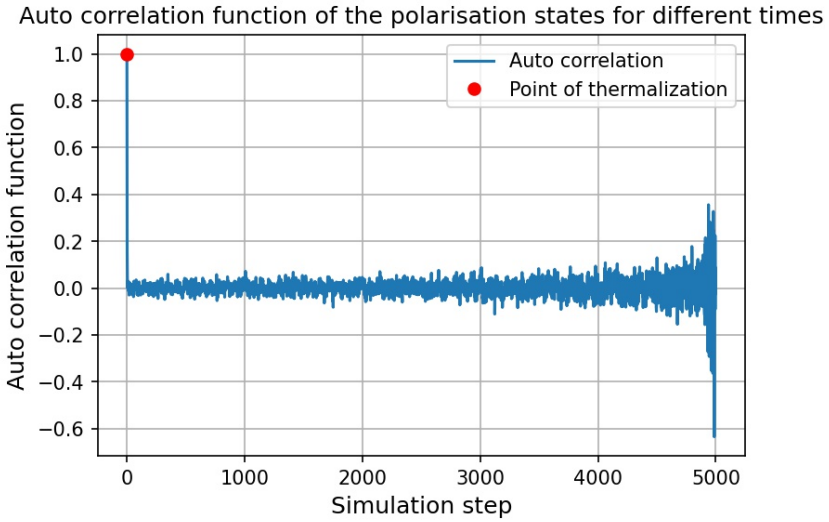

Figure 3: The auto-correlation function of $\eta = 0.80$. The red dot represents the point of thermalization.

The system does not change its behaviour from the start of the simulation, and so is immediately thermalized. Figure (4), shows the $\log(\langle N \rangle)$ vs $\log(\Delta N)$ plot.

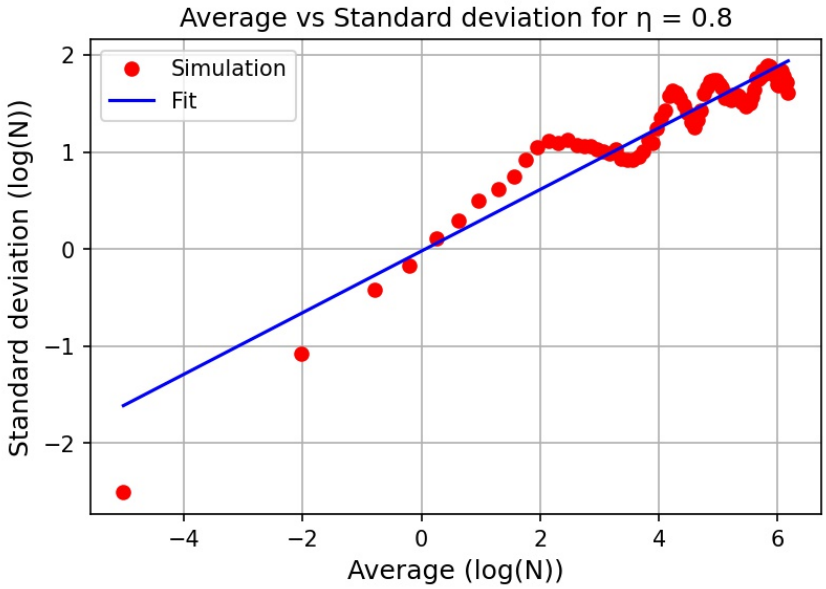

Figure 4: The log-log plot of the average vs the standard deviation for $\eta = 0.30$. The red dots represent the simulation data. The blue line represents the fit of the simulation data.

The slope of the fit is $z = 0.42$.

Repeating the simulations for a range of η's, from 0.00 to 1.00 in steps of 0.05. Figure (5), shows how the z-exponent is depended on the noise η of the system.

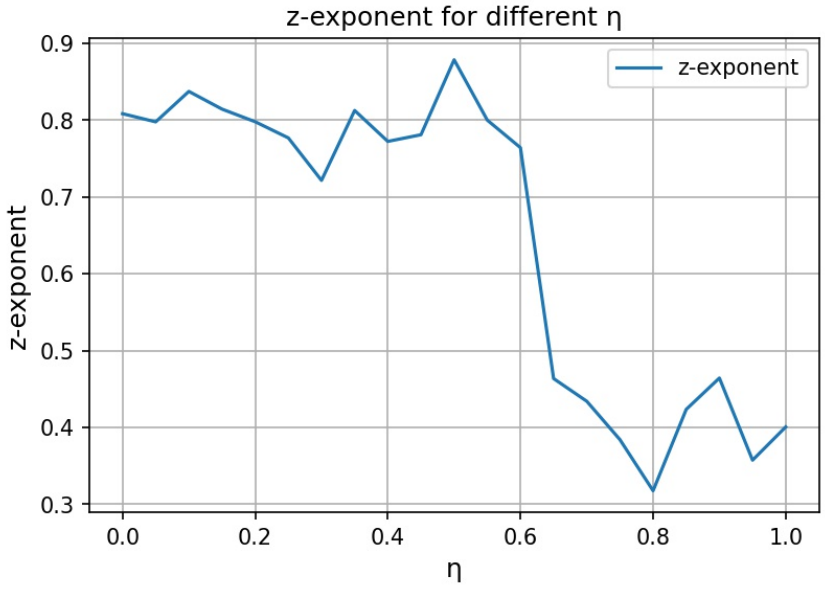

Figure 5: The z-exponent vs the noise η.

There are three interesting regions: The ordered phase, the disordered phase and the phase transition. From figure (5), the ordered phase occurs for values $\eta \leq 0.6$. The phase transition occurs between $\eta = 0.6$ and $\eta = 0.7$. The disordered phase occurs for values $\eta \geq 0.7$. In the ordered phase, the z-exponents have valid values that obey scaling law in Eq.(2). The ordered phase is shown in figure (6).

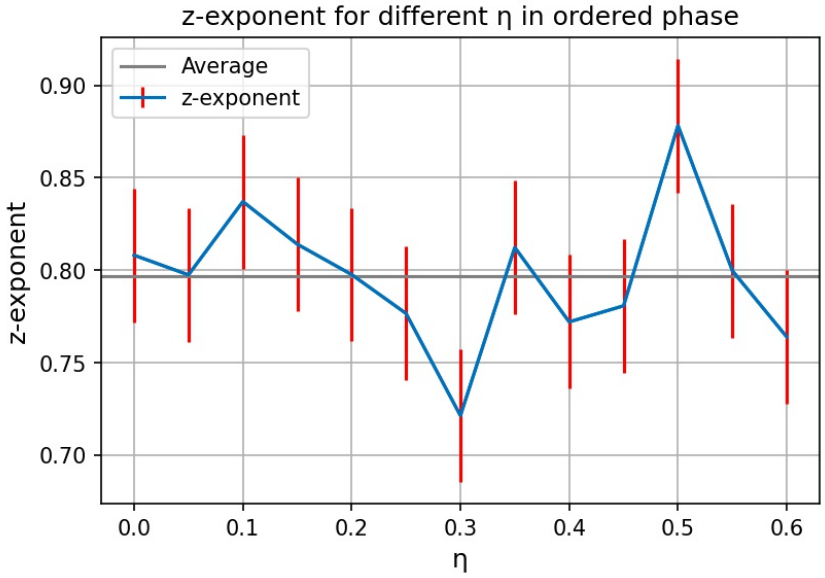

Figure 6: The z-exponent vs the noise η in the ordered phase. The grey line represents the average value of the z-exponent. The blue line represents the simulated values of the z-exponent, with corresponding errors indicated by the red lines.

This yields an average value of the z-exponent in the ordered phase, $z = 0.797 \pm 0.04$. The disordered phase is shown in figure (7).

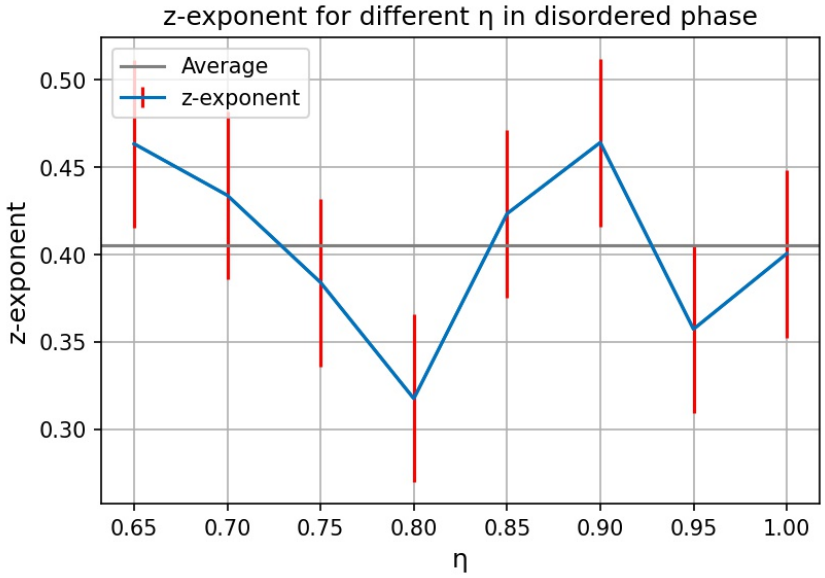

Figure 7: The z-exponent vs the noise η in the disordered phase. The grey line represents the average value of the z-exponent. The blue line represents the simulated values of the z-exponent, with corresponding errors indicated by the red lines.

In the disordered phase, the average z-exponent is $z = 0.41 \pm 0.04$. Continuing with the phase transition, from figure (5) it is clear that it must occur between $\eta = 0.6$ and $\eta = 0.7$. This region is further examined in figure (8), where the values of η range from 0.6 to 0.7 in steps of 0.01.

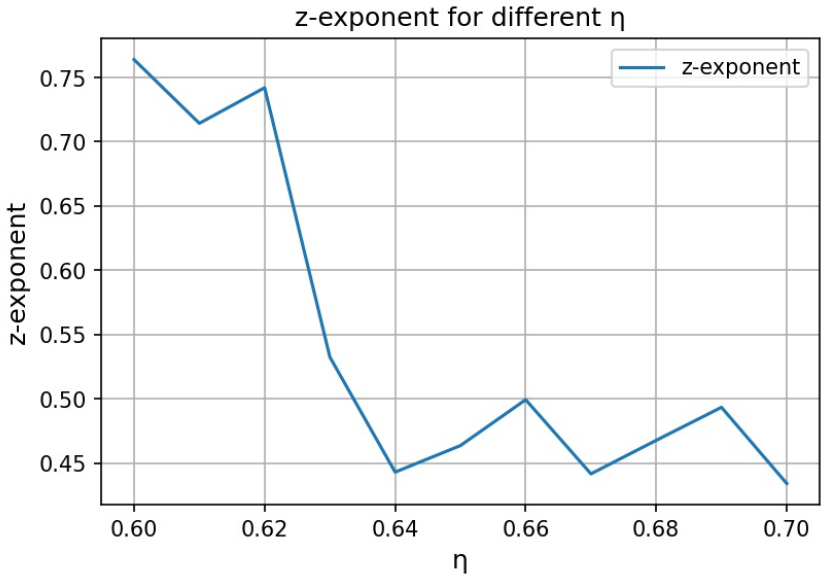

Figure 8: The z-exponent vs the noise η near the transition phase.

The results show a phase transition occurring between $\eta = 0.62$ and $\eta = 0.63$.

4. Discussion and Conclusion

From figure (5), the noise (η) dependence on the z-exponent differs per phase. In the ordered phase, the z-exponent is constant for all values $\eta \leq 0.62$, where $z = 0.797 \pm 0.04$. Whereas, in the disordered phase $z = 0.41 \pm 0.04$. Therefore, the z-exponent is not universal. The difference in the z-exponent arises from the fact that in the disordered phase, the particles orientation is dominated by the noise (η) term. This ensures that the particles cannot properly form collective motion. In the ordered phase, the noise term does not dominate, hence the particles can form collective motion.

Furthermore, the analytical and numerical results are not in agreement. The analytical result is $z = 1$, whereas the numerical result is $z = 0.797 \pm 0.04$ in the ordered phase. When the system has thermalized, the transversal and longitudinal direction of $\boldsymbol{q}$ differ from another, which creates an anystropic structure. The theory does not account for anystropic structure of the number density, and so will give conflicting results compared to the simulation. For the disordered phase, the z-exponent of the simulation ($z = 0.41 \pm 0.04$) does come close to the analytical value ($z = \frac{1}{2}$). Nonetheless, there is a noticable difference. This difference may come from the fact that the number of simulation steps is too small, and the number of simulations performed in both regions is also too small for a complete analysis.

Moreover, the phase transition of the system occurs between a noise level of $\eta = 0.62$ and $\eta = 0.63$. It is unclear from a first look if the phase transition is continuous or discontinuous. Further analysis of both theory and simulation are required to draw any conclusions. Simulation wise, the number of simulation steps can be greatly increased. Together with an increase in the number of simulations performed in the phase transition region.